DOI: 10.1534/genetics.103.025676

Caenorhabditis elegans WASP and Ena/VASP Proteins Play Compensatory Roles in Morphogenesis and Neuronal Cell Migration

Jim Withee, Barbara Galligan, Nancy Hawkins and Gian Garriga[1]

Department of Molecular and Cell Biology, University of California, Berkeley, California 94720-3204

Manuscript received December 11, 2003
Accepted for publication March 18, 2004

ABSTRACT

We report here that WASP and Ena/VASP family proteins play overlapping roles in *C. elegans* morphogenesis and neuronal cell migration. Specifically, these studies demonstrate that UNC-34/Ena plays a role in morphogenesis that is revealed only in the absence of WSP-1 function and that WSP-1 has a role in neuronal cell migration that is revealed only in the absence of UNC-34/Ena activity. To identify additional genes that act in parallel to *unc-34/ena* during morphogenesis, we performed a screen for synthetic lethals in an *unc-34* null mutant background utilizing an RNAi feeding approach. To our knowledge, this is the first reported RNAi-based screen for genetic interactors. As a result of this screen, we identified a second *C. elegans* WASP family protein, *wve-1*, that is most homologous to SCAR/WAVE proteins. Animals with impaired *wve-1* function display defects in gastrulation, fail to undergo proper morphogenesis, and exhibit defects in neuronal cell migrations and axon outgrowth. Reducing *wve-1* levels in either *unc-34/ena* or *wsp-1* mutant backgrounds also leads to a significant enhancement of the gastrulation and morphogenesis defects. Thus, *unc-34/ena*, *wsp-1*, and *wve-1* play overlapping roles during embryogenesis and *unc-34/ena* and *wsp-1* play overlapping roles in neuronal cell migration. These observations show that WASP and Ena/VASP proteins can compensate for each other *in vivo* and provide the first demonstration of a role for Ena/VASP proteins in gastrulation and morphogenesis. In addition, our results provide the first example of an *in vivo* role for WASP family proteins in neuronal cell migrations and cytokinesis in metazoans.

DRAMATIC and often rapid changes in filamentous actin (F-actin) abundance and distribution are essential for a range of cellular processes, including cell polarity, vesicular trafficking, cytokinesis, and cellular movements (Carlier *et al.* 2003). A large number of activities that regulate F-actin abundance and distribution have been described and many of them attributed to proteins that are evolutionarily conserved. Although many of these activities are well characterized *in vitro*, their exact role *in vivo* is still unclear in many instances.

The Ena/VASP proteins constitute a family of evolutionarily conserved actin-regulating proteins that act in many cellular processes, including axon guidance, phagocytosis, adhesion, and intracellular movement of the *Listeria monocytogenes* pathogen (Gertler *et al.* 1990, 1996; Lanier *et al.* 1999; Laurent *et al.* 1999; Vasioukhin *et al.* 2000). Ena /VASP proteins promote actin filament elongation and bundling *in vitro* and are thought to link signaling pathways to F-actin remodeling *in vivo*. This protein family shares three conserved domains: an N-terminal Ena/VASP homology I domain (EVH1), a central proline-rich domain (PRD), and a C-terminal Ena/VASP homology II (EVH2 domain; Reinhard *et al.* 2001; Kwiatkowski *et al.* 2003; Figure 1). The EVH1 domain binds the consensus motif (D/E)-FFPPPP-X(D/E)(D/E) and is sufficient to target Ena/VASP proteins to focal adhesions and to Listeria (Gertler *et al.* 1996; Niebuhr *et al.* 1997; Ahern-Djamali *et al.* 1998). The central PRD binds several known SH3-domain-containing proteins as well as the actin exchange factor profilin (Gertler *et al.* 1995, 1996; Reinhard *et al.* 1995). Finally, the C-terminal EVH2 domain binds globular and F-actin and is required for multimerization (Bachmann *et al.* 1999). Previous work in fibroblast cells *in vitro* supports a model where Ena/VASP proteins promote F-actin elongation by binding free filament ends and by inhibiting the activity of capping proteins that prevent filament extension (Bear *et al.* 2002).

WASP family proteins also promote F-actin formation but utilize a different mechanism from Ena/VASP proteins. WASP family proteins catalyze the formation of new F-actin branches from existing filaments and are divided into three protein subfamilies: WASP, N-WASP, and SCAR/WAVE proteins (Pollard *et al.* 2000; Badour *et al.* 2003; Carlier *et al.* 2003). All three subfamilies share a conserved C terminus, the VCA region (verprolin, cofilin homology, acidic region), as well as a central PRD. The VCA domain interacts directly with the ARP2/3 complex and globular actin to catalyze the formation of new F-actin branches from existing filaments (Blanchoin *et al.* 2000; Pantaloni *et al.* 2000; Amann and Pollard 2001), and the PRD binds SH3 domain proteins as well

[1]*Corresponding author:* Department of Molecular and Cell Biology, 401 Barker Hall, University of California, Berkeley, CA 94720-3204. E-mail: garriga@uclink4.berkeley.edu

as profilin (Rivero-Lezcano *et al.* 1995; Miki *et al.* 1997; Suetsugu *et al.* 1999a). The N termini of WASP and SCAR/WAVE proteins, on the other hand, differ substantially (Figure 1). WASP and N-WASP proteins contain an N-terminal EVH1 domain and a more central regulatory region. The EVH1 domain binds a conserved proline-rich motif and may be important for the subcellular localization of WASP proteins (Niebuhr *et al.* 1997; Ramesh *et al.* 1997; Prehoda *et al.* 1999), while the regulatory region binds the activators CDC42 and PIP2 (Aspenstrom *et al.* 1996; Symons *et al.* 1996; Rohatgi *et al.* 2000). SCAR/WAVE proteins, on the other hand, are characterized by an N-terminal SCAR homology domain and are regulated and localized by different mechanisms (Miki *et al.* 1998b; Suetsugu *et al.* 1999b).

Despite the fact that they affect F-actin remodeling through distinct mechanisms, Ena/VASP and WASP family proteins share several features. First, both Ena/VASP and WASP proteins contain the EVH1 and PRD domains and have been shown to bind profilin directly through their respective PRD (Figure 1). Second, both associate directly with globular actin. Finally, both are localized to sites of actin polymerization in response to cellular signals and are thought to be important for F-actin remodeling in response to extracellular cues (Bashaw *et al.* 2000; Castellano *et al.* 2001; Suetsugu *et al.* 2002; Kwiatkowski *et al.* 2003). Interestingly, WASP and VASP proteins interact *in vitro*, and VASP may be required for WASP to activate the ARP2/3 complex at the periphery of hemopoietic cells (Castellano *et al.* 2001).

We have characterized the *in vivo* roles of Ena/VASP and WASP family proteins in the nematode *Caenorhabditis elegans* using a combination of traditional genetic analysis and a functional, RNA interference (RNAi)-based screen for synthetic lethality in an *unc-34* mutant background. We report that the *C. elegans* Ena homolog plays a role in morphogenesis revealed only in the absence of either *wsp-1* or *wve-1* (the *C. elegans* homologs of WASP and WAVE, respectively). In addition, *wsp-1* plays a role in neuronal cell migration revealed only in the absence of *unc-34/ena*. We also provide *in vivo* evidence that *wve-1* is required for proper neuronal cell migration and axon outgrowth. Finally, we show that *wsp-1* is required for proper cytokinesis during embryogenesis. This is the first time, to our knowledge, that WASP family proteins have been implicated in cytokinesis in a metazoan.

MATERIALS AND METHODS

***C. elegans* genetics:** *C. elegans* were cultured as described (Brenner 1974). Worms were grown at 20° except where noted otherwise. Mutations used in this study were *wsp-1(gm324)* (LGIV) and *unc-34(e315)* and *unc-34(gm104)* (LGV). The *unc-34(gm104)* allele used in this study is a null mutation by several criteria. *gm104* has been sequenced and contains an early amber stop at W24. In addition, staining of *unc-34(gm104)* mutant embryos or probing of Western blots from mutant extracts produced no detectable signal. Finally, extensive comparison of the cell migration and axon outgrowth defects in *unc-34(gm104)* to a mutant that lacks the *unc-34* genomic region has detected no discernible differences in the penetrance or expressivity between the two (G. Garriga and M. Dell, unpublished results).

We constructed *wsp-1(gm324)/mIs12*; *unc-34(gm104)* strains to analyze the *wsp-1(gm324)*; *unc-34(gm104)* double mutants. *mIs12* is an array of *myo-2*::GFP, *pes-10*::GFP, and F22B7.9::GFP integrated on LGIV that acted as a balancer of *wsp-1(gm324)* in these studies. *wsp-1; unc-34* double mutants from *wsp-1/mIs12*; *unc-34* parents were identified by a lack of green fluorescent protein (GFP) expression.

Phenotypic characterizations: *Embryonic lethality:* All embryonic lethality was quantified at 25° because the *wsp-1* mutant and *wve-1* RNAi induced more severe lethality at this temperature. To quantify embryonic lethality, 10 young adults were transferred to a new plate. After laying embryos for 5–8 hr, the parents were removed and the embryos counted under a dissection microscope. The embryos were then incubated for 24 hr at 25° and counted again. The percentage of unhatched embryos after 24 hr was reported as the percentage of embryonic lethal. All strains were quantified at least three times with an N of ~100 each time.

Brood size measurements: Brood size measurements were all performed at 25° since both *wsp-1* and *unc-34* mutants exhibited the most severe defect at this temperature. Brood sizes were calculated by transferring an L4 hermaphrodite to a new plate every 12 hr and counting the number of embryos laid for each 12-hr period until no more progeny were produced, typically ~48–60 hr at 25°. Brood sizes were counted for 20 parents of each genotype reported.

Four-dimensional microscopy: Time-lapse microscopy in multiple focal planes was performed for analysis of embryogenesis and cytokinesis defects. All microscopy was performed at ~22° using a ×63 lens on a Zeiss Axioskop 2 mot plus microscope with a Hamamatsu ORCA-ER camera automated by Open Lab software. Embryos were mounted for microscopy by cutting open hermaphrodites with a 27G needle and mouth pipetting them in M9 media to a 4% agar pad. The coverslip was sealed with molten Vaseline to prevent evaporation. Time points were collected either every 30 sec or every minute in three to five 2-μm sections/time point.

Cell migration and axon outgrowth: The extent of neuronal cell migration in wild-type and mutant worms was determined by Nomarski optics for the anterior lateral microtubule neuron, canal-associated neuron (CAN), and hermaphrodite-specific neuron as previously described (Wightman *et al.* 1996). Axon morphology was assessed in L1 larvae mounted on 4% agar pads in M9 + 50 mm NaN_3 with the integrated *unc-25*::GFP DD motor axon reporter *juIs76*.

RNA interference: For double-stranded RNA interference (dsRNAi), of *wsp-1*, a 1-kb *Sac*I fragment of yk184g1 (provided by Y. Kohara at the National Institute of Genetics, Mishima, Japan) was cloned into the vector L4440. L4440 contains opposing T7 polymerase binding sites that allow production of double-stranded RNA (dsRNA) within bacteria for RNAi feeding experiments. We also used this same vector to produce dsRNA from *in vitro* transcription reactions for RNAi injection. The clone JA:R06C1.3 was used for *wve-1* RNAi feeding and injection experiments (Fraser *et al.* 2000). RNAi feeding experiments were performed as follows. HT115 bacteria (Timmons *et al.* 2001) containing L4440 with or without an insert were grown overnight at 37° in Luria broth (LB) + 25 μg/ml carbenicillin and spotted on NGM plates + 25 μg/ml carbenicillin + 1 mm isopropyl thiogalactoside (IPTG) and incubated at 22° for 12 hr. L3 hermaphrodites were transferred to the above NGM plates and allowed to feed at 15° for 48–54

hr and then transferred to a new NGM plate prepared as described above. Worms were allowed to lay embryos for 8–12 hr at 25° and embryonic lethality was quantified as described above. Neither *wsp-1* nor *wve-1* RNAi feeding produced any significant embryonic lethality in wild-type worms. However, feeding either *wsp-1* or *wve-1* dsRNA to *unc-34* mutants or feeding *wve-1* dsRNA to the *wsp-1* mutant resulted in ~60–80% lethality. For simplicity the results reported here are from RNAi into *unc-34(gm104)*; however, a comparable level of embryonic lethality was induced by both *wsp-1* and *wve-1* dsRNA fed to three different *unc-34* null alleles [*unc-34(gm104)*, *unc-34(e951)*, and *unc-34(gm114)*].

dsRNA for injection was produced by linearizing the appropriate L4440 construct to allow *in vitro* RNA synthesis of the plus and minus strands in independent reactions [Promega (Madison, WI) RiboMAX RNA production system]. The single-stranded products were hybridized in injection buffer (20 mM KPO_4 pH 7.5, 3 mM potassium citrate, 2% polyethylene glycol 6000) by incubating at 68° for 10 min followed by a 30-min incubation at 37°. dsRNA was injected into the gonad or intestine at 0.5–1.0 μg/μl. Injected parents were incubated 12–15 hr at 25° and then either transferred to a new plate at 25° to quantify embryonic lethality or utilized for 4D microscopy.

RNAi feeding screen: We screened a library corresponding to 2445 genes from LGI (Fraser *et al.* 2000) for RNAi clones that created significantly more embryonic lethality in an *unc-34* mutant background than in a wild-type background. Bacteria were inoculated into 100 μl of LB + 25 μg/ml carbenicillin using a 96-well format replicator and grown 8 hr at 37°. A total of 10 μl of each strain was then spotted to three NGM plates + 25 μg/ml carbenicillin + 1 mM IPTG (in a 12-well format) and incubated at room temperature for 12–15 hr. To prepare worms for RNAi feeding, gravid hermaphrodites were treated with a solution of 0.2% NaOCl and 0.7 M NaOH to release embryos. Embryos were then transferred to a fresh NGM plate without bacteria and incubated at 20° for 24 hr to allow them to hatch and to arrest as a synchronized population of L1 larvae. L1 larvae were then transferred to NGM plates with bacteria and allowed to mature to a synchronized population of L3/L4 worms for ~24 hr at 20°. L3/L4 worms were washed from the plate and resuspended in M9 media to a titer of ~25 worms/3 μl of M9. A total of 3 μl of this worm suspension was spotted to one of the three NGM carbenicillin IPTG plates for a given bacterial strain, prepared as described above, and incubated at 15°. After 50–54 hr, six worms from the original plate were transferred to the two remaining plates for a given bacterial clone and incubated at 25° to assess embryonic lethality as described above. Worms were shifted to 25° to assess embryonic lethality because we reasoned that other synthetic lethal RNAi clones might show the same enhancement at higher temperatures exhibited by *wsp-1* RNAi. Thus, all bacterial clones were checked in duplicate for their effect on embryonic lethality to help with the variable results inherent to the RNAi feeding (Simmer *et al.* 2003).

Using our methodology we successfully screened 2244 clones from the LG1 library for embryonic lethality in an *unc-34(gm104)* background. All clones that gave significantly higher embryonic lethality in the *unc-34* mutant than previously reported for wild type were retested on wild type. We found lethality associated with ~80% of the clones previously reported to cause embryonic lethality and an additional 21 clones not previously reported to cause lethality in wild type. We also identified 9 clones that conferred more lethality in *unc-34* than in wild type and report on one of those clones here (see RESULTS). The remaining 8 clones were not further characterized because they gave inconsistent embryonic lethality in the *unc-34* mutant upon retesting.

Identification of *wsp-1* deletion allele: A library representing ~900,000 haploid genomes of UV-trimethylpsoralen mutagenized worms was created by a consortium of postdocs and graduate students at the University of California, Berkeley, on the basis of protocols established by Bob Barstead's lab, the nemaPharm Group at Axis Pharmaceuticals, and Ron Plasterk's lab and modified and communicated by Micheal Koelle, Heather Hess, and David Shechner (http//info.med.yale.edu/mbb/koelle/protocol_Gene_knockouts.html). We screened the library for deletions that span the *wsp-1* genomic region using three sets of overlapping, nested primer pairs that cover the entire genomic region and identified a single *wsp-1* deletion allele using the nested primer pairs (CATTTCGCTC AGTTTTCTCG, TTTTGACGAAACCATTGATCC) and (CAC CAAAATTATTAGTTAGGGATAAGG, CAATTAGTTTTGCC GTTTTCG). The deletion begins in exon II and ends in the third intron removing nucleotides 470–2329 of the *wsp-1* gene.

Anti-wsp-1 antibodies and *wsp-1* RT-PCR: A 354-bp fragment from the VCA domain of *wsp-1* was amplified to introduce *Bgl*II/*Eco*RI sites using the primer pair (AGATCTTCGGTGCT CGCAAAACTAC) and (GAATTCCTAATCTGACCATTCATT TTTGTCATC). The PCR product was digested with *Bgl*I/*Eco*RI and cloned into pGEX4T.2 (Amersham, Buckinghamshire, UK) to create a glutathione *S*-transferase fusion that was purified from bacteria using standard techniques and injected into rabbits and rats. A maltose binding protein-VCA fusion was created using the vector pMAL-c2 (New England Biolabs, Beverly, MA) from the same *Bgl*II/*Eco*RI fragment above and used for affinity purification of antisera [Pierce (Rockford, IL) SulfoLink coupling gel]. Affinity-purified fractions were used for immunoblotting, utilizing standard techniques. Anti-WSP-1 from rabbits and rats recognized a single, 65-kD band in embryo extracts not present in *wsp-1(gm324)*. Although we tried several different protocols, we were unable to observe a specific immunostaining pattern in embryos or in mixed-stage worms using these antibodies.

PCR amplification of *wsp-1* cDNA fragments was performed on cDNAs created from wild-type and *wsp-1*(*gm324*) embryos using standard methods for mRNA isolation and poly(dT) oligo for reverse transcription. Three primer pairs that span different regions of the *wsp-1* cDNA were then used to amplify *wsp-1* specific sequences from wild-type or *wsp-1(gm324)* cDNAs. All three primer pairs contain sequences specific to *wsp-1* that are not removed by the deletion in *wsp-1(gm324)*. The sequences of the primers used to generate Figure 1 were (GCACAAGTT TTACAAATTCGTCACTTTCAAATG) and (ATGCTTTTCGC TTTGGTCGG). The other two primer pairs were more C-terminal and correspond to sequences found in the PRD and VCA domains, respectively. In addition, primers specific to an α-tubulin gene (*tba-1*) were used for PCR amplification on the cDNAs from both wild type and *wsp-1(gm324)* as a control.

RESULTS

A *C. elegans* N-WASP homolog can compensate for a lack of *unc-34/ena* during embryogenesis: The *unc-34* gene encodes the sole Enabled homolog in the *C. elegans* genome and is hereafter referred to as *unc-34/ena* (Figure 1; Yu *et al.* 2002; M. Dell, W. Forrester, F. Gertler, H. R. Horvitz and G. Garriga, unpublished results). Because Ena/VASP proteins are known to mediate cell movement and adhesion in several systems, we asked whether *unc-34/ena* plays a role in *C. elegans* embryonic morphogenesis.

Careful examination of *unc-34/ena* mutant embryos revealed no significant lethality or obvious defects in

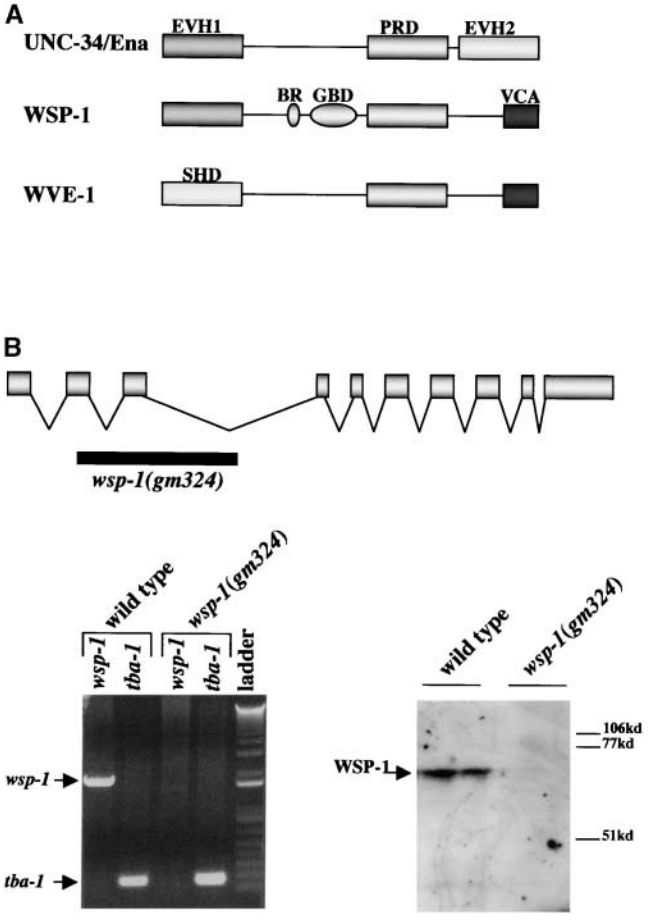

FIGURE 1.—(A) UNC-34/Ena, WSP-1, and WVE-1 similarities. *unc-34/ena* and *wsp-1* encode homologs of Ena/VASP and WASP proteins, respectively. Both proteins have an N-terminal EVH1 domain that binds a proline-rich consensus and a PRD known to bind SH3-containing proteins and profilin. In addition, UNC-34/Ena has a C-terminal domain EVH2 required for F-actin binding and multimerization while WSP-1 contains the *b*asic *r*egion (BR) and *G*TPase *b*inding *d*omain (GBD), which bind PIP2 and CDC42, respectively, to regulate activity. *wve-1* encodes a homolog of SCAR/WAVE proteins. WVE-1 lacks an EVH1 domain but contains two domains found in WASP family proteins: a PRD and a C-terminal VCA region known to bind and activate the actin-nucleating complex ARP2/3. (B) The *wsp-1(gm324)* deletion mutant contains no detectable *wsp-1* message or protein. *wsp-1(gm324)* spans nucleotides 470–2329 beginning in exon II and ending in intron III. (Lower left) PCR amplification products from primers specific to *wsp-1* or *tba-1* (as a control) using cDNAs from either wild-type or *wsp-1(gm324)* animals as a template (see MATERIALS AND METHODS). Although primers specific to *tba-1* (used as a control) amplified the predicted product from both wild type and *wsp-1(gm324)*, *wsp-1*-specific primers amplified a product only from wild-type cDNA. (Lower right) A Western blot performed on extracts from wild-type and *wsp-1(gm324)* mutant embryos (see MATERIALS AND METHODS). Anti-WSP-1 recognizes the predicted 65-kD band in wild-type but not in *wsp-1(gm324)* extracts.

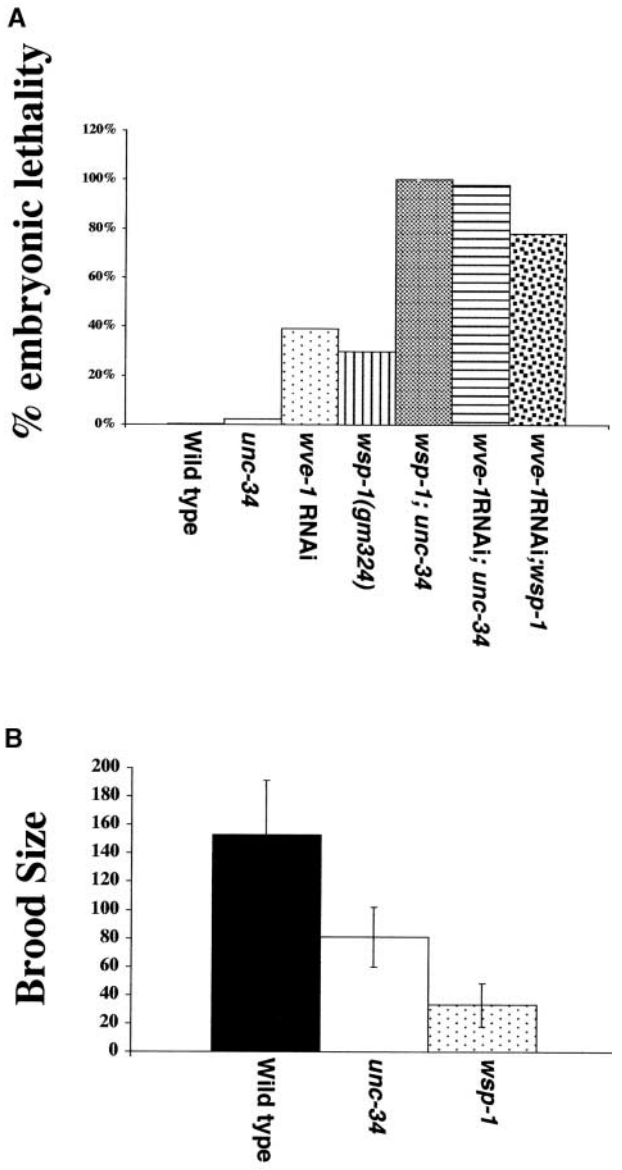

FIGURE 2.—Embryonic lethality and brood sizes measured at 25°. (A) Percentage of embryonic lethality of wild type, *unc-34(gm104)*, *wve-1* RNAi, *wsp-1(gm324)*, *wsp-1; unc-34 (gm104)*, *wve-1* RNAi; *unc-34(gm104)*, and *wve-1* RNAi; *wsp-1(gm324)*. All $N \geq 200$; percentage of embryonic lethality was determined as described in MATERIALS AND METHODS. Note that reducing either WSP-1 or WVE-1 in an *unc-34* mutant background confers a significant increase in embryonic lethality ($P < 0.0001$, two-tailed *z*-test) In addition, reducing WVE-1 in a *wsp-1* mutant background also leads to a significant increase in lethality ($P < 0.0001$, two-tailed *z*-test). (B) Brood sizes of wild-type, *unc-34(gm104)*, and *wsp-1(gm324)* hermaphrodites. Brood size is defined as the total number of embryos, viable and inviable, produced over the life time of a single hermaphrodite; 20 independent hermaphrodites were measured for each genotype as described in MATERIALS AND METHODS.

embryogenesis, although we did observe a decreased brood size from *unc-34/ena* mutant hermaphrodites (Figure 2). Thus, either *unc-34/ena* plays no role in embryogenesis or other proteins are sufficient for proper embryogenesis in its absence.

We reasoned that proteins with homology to Ena/VASP family members were good candidates for activi-

ties that might compensate for a lack of *unc-34/ena* during embryogenesis. Although the *C. elegans* genome contains only a single Ena/VASP homolog, two additional *C. elegans* genes encode proteins with EVH1 domains: B0280.2 on chromosome III and the *C. elegans* N-WASP homolog *wsp-1* on chromosome IV. To test whether these proteins might have overlapping roles with *unc-34/ena* during embryogenesis, we injected dsRNAi corresponding to each of the above genes into wild-type and *unc-34/ena* mutant worms (MATERIALS AND METHODS). RNAi of B0280.2 caused ~8% embryonic lethality that was not enhanced by mutations in *unc-34/ena*. Consistent with previous experiments (SAWA *et al.* 2003), we found RNAi of *wsp-1* caused a moderate amount of embryonic lethality corresponding to 19% ($N = 324$) as well as a reduced brood size (our unpublished results). Interestingly, *wsp-1* RNAi into an *unc-34/ena* mutant increased the embryonic lethality to 100% ($N = 200$). Thus, *unc-34/ena* and *wsp-1* compensate for each other during embryogenesis.

To further characterize the *wsp-1* phenotype and the genetic interaction between *wsp-1* and *unc-34/ena*, we isolated a deletion mutant of *wsp-1* (MATERIALS AND METHODS). The deletion *wsp-1(gm324)*, which removes nucleotides 470–2329 of the *wsp-1* gene, begins in exon II and ends in the third intron (Figure 1B; MATERIALS AND METHODS). We performed PCR amplification using primers to several portions of *wsp-1* cDNA from mRNA extracted from wild-type or *wsp-1(gm324)* embryos. Although we were able to amplify products of the predicted molecular weight from wild-type cDNAs in each case, we were unable to amplify visible products from the *wsp-1* mutant (Figure 1B; MATERIALS AND METHODS). We also raised antibodies to a C-terminal portion of WSP-1 that detected a single 65-kD band in extracts of wild-type embryos but no detectable protein from *wsp-1(gm324)* animals (Figure 1B; MATERIALS AND METHODS). On the basis of these results and the nature of the deletion, we believe that *wsp-1(gm324)* is likely to contain very little or no *wsp-1* activity.

wsp-1(gm324) had a set of phenotypes qualitatively similar to those reported for *wsp-1* RNAi, including 25% embryonic lethality and a greatly reduced brood size (Figure 2, A and B). The embryonic lethality of *wsp-1(gm324)* was enhanced at higher temperatures (MATERIALS AND METHODS). Because we were unable to detect protein or mRNA in *wsp-1(gm324)* mutants, we do not believe that *gm324* is temperature sensitive. Instead, removing *wsp-1* function appears to reveal a temperature-sensitive process required for embryogenesis.

wsp-1; *unc-34/ena* double mutants from *wsp-1*/+; *unc-34* parents reach adulthood as sick, egg-laying-defective animals with greatly reduced brood sizes—<10 embryos/animal on average—and no surviving embryos (Figure 2; MATERIALS AND METHODS). Thus, *unc-34/ena* is absolutely required for embryogenesis in the absence of *wsp-1*, and maternally provided *wsp-1* rescues the embryonic lethal phenotype of *wsp-1*; *unc-34/ena* mutant embryos. It is noteworthy that the phenotype of *unc-34/ena* mutants treated with *wsp-1* RNAi is consistent with the *wsp-1*; *unc-34/ena* double-mutant phenotypes since RNAi treatment removes both the zygotic and the maternal mRNA contributions.

***wsp-1* and *unc-34/ena* are required for morphogenesis:** During *C. elegans* embryogenesis hypodermal cells are born on the dorsal side of the embryo and migrate ventrally to form adherens junctions on the ventral side in a process known as ventral or hypodermal enclosure (SULSTON *et al.* 1983; WILLIAMS-MASSON *et al.* 1997, 1998; SIMSKE and HARDIN 2001). Once the embryo is properly enclosed, circumferential actin bands contract and transform the ovoid embryo into the elongated shape of a worm (PRIESS and HIRSH 1986). Embryos that fail to enclose properly extrude internal tissues during elongation and die before or shortly after hatching. Ventral enclosure also requires the proper execution of earlier stages of embryogenesis, including gastrulation. During *C. elegans* gastrulation, gut, germline, and mesoderm precursors ingress on the ventral side of the embryo, leaving small depressions or clefts on the ventral surface that are closed by short movements of the neighboring cells (SULSTON *et al.* 1983; NANCE and PRIESS 2002). In particular, ingression of the embryonic founder cell MS cell descendants results in a more persistent cleft, typically referred to as the ventral cleft, which is usually closed by neighboring neuroblasts ~60–100 min before ventral enclosure (NANCE and PRIESS 2002). Closure of the ventral cleft may be required for proper ventral enclosure since disruption of these neuroblast movements results in large, persistent ventral clefts and a corresponding failure in ventral enclosure later in embryogenesis (GEORGE *et al.* 1998; CHIN-SANG *et al.* 1999, 2002; CHIN-SANG and CHISHOLM 2000; HARRINGTON *et al.* 2002). Hereafter we refer to the processes of gastrulation and ventral enclosure collectively as morphogenesis.

To determine when *wsp-1* and *unc-34/ena* function during embryogenesis, we analyzed *wsp-1* mutant embryos and *wsp-1*; *unc-34/ena* double-mutant embryos by 4D microscopy (MATERIALS AND METHODS). As discussed above, ~25% of *wsp-1(gm324)* embryos die at 25° (Figure 2A). We found that ~50% of this lethality is associated with a failure of the hypodermal cells to migrate and/or to form junctions properly during hypodermal enclosure (Figure 3). In addition, we report here for the first time that *wsp-1* is required for multiple aspects of embryogenesis that occur well before enclosure (see below and Figures 3 and 6). In some instances these earlier defects are sufficient to confer lethality prior to hypodermal enclosure. We first describe *wsp-1*; *unc-34/ena* defects in morphogenesis and then discuss the earlier phenotypes.

Approximately 60–70% of the time *wsp-1* mutant embryos exhibited enlarged, persistent ventral clefts relative to wild type (Figure 3). Although these aberrant

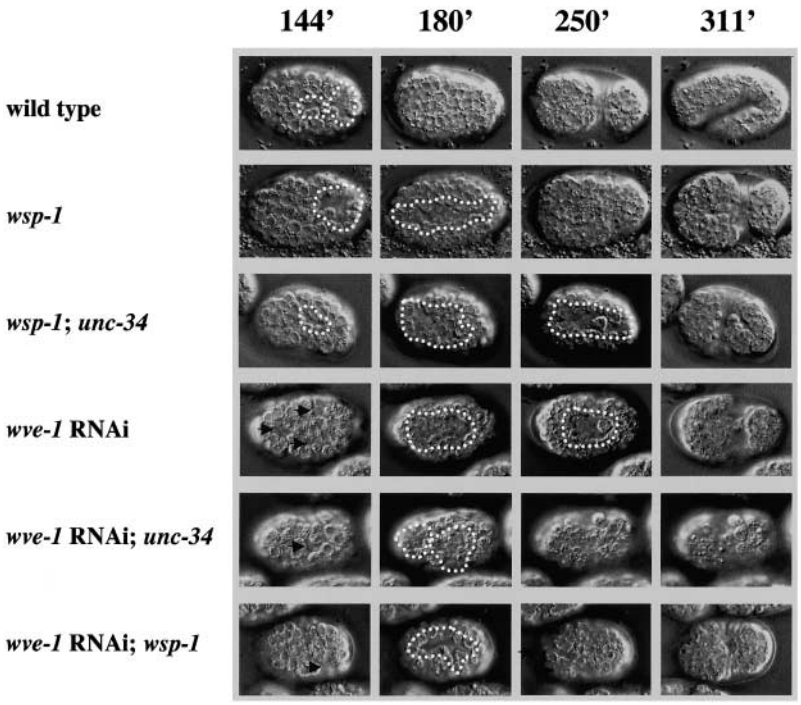

FIGURE 3.— 4D microscopy of morphogenesis in wild type, *wsp-1*, *wsp-1*; *unc-34*, *wve-1* RNAi, *wve-1* RNAi; *unc-34*, and *wve-1* RNAi; *wsp-1* mutant embryos (see MATERIALS AND METHODS). Time series from six different embryos are shown in minutes after the first cell division. All panels are ventral views with anterior to the left except the wild-type embryo at 311 min, which is lateral. Ventral clefts are marked with a dotted white line. Irregularities in the ventral surface induced by *wve-1* RNAi are marked with arrows. 144 min: Ventral clefts are approximately equivalent for all genotypes at 144 min after the first cell division except for the *wve-1* RNAi treatment (see RESULTS for details). 180 min: By 180 min *wsp-1*, *wsp-1*; *unc-34 (gm104)*, *wve-1* RNAi, *wve-1* RNAi; *unc-34(gm104)*, and *wve-1* RNAi; *wsp-1* embryos exhibit greatly enlarged ventral clefts while the wild-type cleft has already closed. 250 min: Wild-type and *wsp-1* embryos have successfully closed ventral clefts and wild type has just completed ventral enclosure while the *wsp-1* embryo is still attempting enclosure. *wsp-1*; *unc-34*, *wve-1* RNAi, *wve-1* RNAi; *unc-34*, and *wve-1* RNAi *wsp-1* embryos show disorganized ventral surfaces with enlarged or misplaced clefts that have persisted well beyond the cleft in the wild-type embryo. 311 min: The wild-type embryo has elongated almost to the two-fold stage. The *wsp-1* embryo has completed epidermal enclosure but exhibits a severe anterior bulge. *wsp-1*; *unc-34*, *wve-1* RNAi, *wve-1* RNAi; *unc-34*, and *wve-1* RNAi; *wsp-1* embryos failed to properly enclose and exhibit severe anterior and posterior bulges.

clefts may result in occasional failures in hypodermal cell migration, they were always closed by the time hypodermal cells began to appear on the ventral surface. *wsp-1* mutants also exhibited a slight delay in embryogenesis. Although wild-type embryos were between 1.5- and 2-fold stages 311 min after the first cell division in our experiments, *wsp-1* embryos were typically between 1- and 1.5-fold at this same time point (Figure 3). Because the cell cycle length of *wsp-1* mutant embryos appeared indistinguishable from wild type during early cell divisions (our unpublished observation), we believe that the delay in *wsp-1* embryogenesis is likely due to defective morphogenesis.

As discussed above, we observed no defects during gastrulation or ventral enclosure of *unc-34/ena* mutant embryos. On the other hand, embryos lacking both maternal and zygotic *unc-34/ena* and *wsp-1* (referred to as *unc-34*$^{m-z-}$; *wsp-1*$^{m-z-}$) die 100% of the time either before or shortly after hypodermal enclosure (Figures 1 and 3). In the majority of *unc-34*$^{m-z-}$; *wsp-1*$^{m-z-}$ mutants we observed large ventral clefts persisting until the time of ventral enclosure (Figure 3). The ventral clefts of *unc-34/ena*; *wsp-1* double-mutant embryos were larger than those in either wild type or *wsp-1* and nearly always persisted until the time of ventral enclosure. The increased persistence of ventral clefts in the *wsp-1*; *unc-34/ena* double-mutant embryos might contribute to the dramatic increase in the ventral enclosure defect.

***wsp-1* is required for proper embryo shape and cytokinesis:** In addition to the large ventral clefts, failures in ventral enclosure and delayed development described above, *wsp-1* mutant embryos also exhibit defects in overall embryo shape. Some of the aberrant embryos are small and round while others are triangular in shape (Figure 4A). These misshapen embryos nearly always fail to hatch, some dying without reaching the stage of hypodermal enclosure.

Approximately 5–10% of *wsp-1* mutant embryos also display a defect in one or more cell divisions (Figure 4B). In some cases the embryos failed in the first cell division and formed single-celled, multinucleate embryos. In other cases the failure in cytokinesis occurs later in development, leading to the formation of a multinucleate cell within an otherwise normal embryo. In most cases where cytokinesis failed, a cleavage furrow initiated normally but the furrow regressed, leading to formation of a multinucleate cell (Figure 4B). Occasionally no visible furrow formed and the cell underwent karyokinesis to produce a multinucleate cell. Embryos with one or more failed divisions invariably died, sometimes without initiating proper gastrulation or morphogenesis. Mutations in *unc-34/ena* appear to enhance the frequency and severity of embryo-shape defects but not the cytokinesis defects of *wsp-1* mutants (our unpublished observation).

***wve-1*, another WASP family protein, plays overlapping roles with both *wsp-1* and *unc-34/ena* during embryogenesis:** To identify other proteins that might overlap in function with UNC-34/Ena during morphogenesis, we performed an RNAi-based screen for genes required for embryonic viability specifically in an *unc-34/ena* mutant background (MATERIALS AND METHODS). Screening an RNAi feeding library that represents 2445 genes from

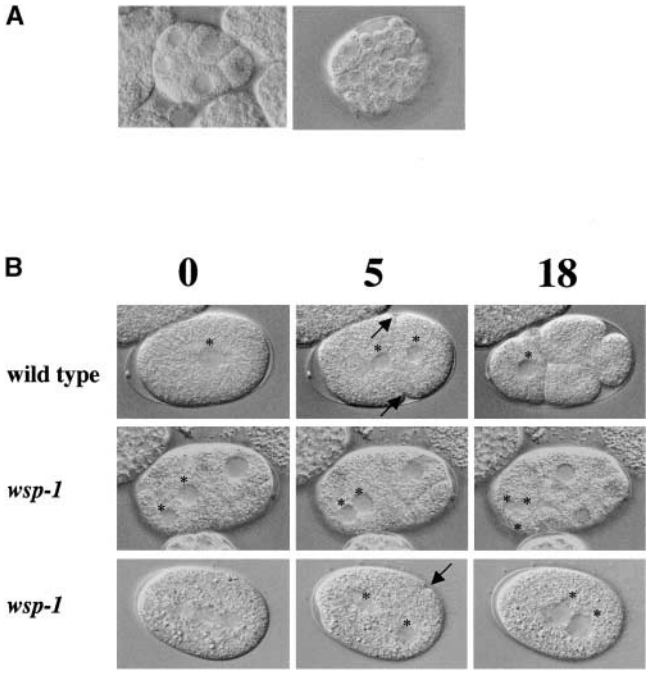

FIGURE 4.—The *wsp-1* mutant displays cytokinesis and embryo-shape defects. (A) *wsp-1* embryos are occasionally misshapen: a triangular and a small, round embryo are shown (left and right, respectively). (B) Time-lapse microscopy showing *wsp-1* cytokinesis defects. Time is in minutes and 0 min is an arbitrary start point. Nuclei are marked with an asterisk and cleavage furrows by an arrow. (First row) A wild-type embryo from fertilization (0 min) to the four-cell stage (18 min). (Second row) A *wsp-1* mutant embryo that contains two nuclei within a single cell in a four-cell embryo at 0 min. The nuclei move together at 5 min and then undergo another round of karyokinesis without cytokinesis by 18 min to form three nuclei in a single cell. (Third row) A *wsp-1* single-celled embryo that forms a spindle at 0 min, a shallow cleavage furrow and two nuclei at 5 min and then two juxtaposed nuclei in a single cell at 18 min.

chromosome I (FRASER *et al.* 2000) yielded several clones that produced a moderate degree of lethality in an *unc-34/ena* mutant background but exhibited either no effect or a mild lethality in wild type (see MATERIALS AND METHODS for details). We identified a single clone that produced 100% embryonic lethality when fed to an *unc-34/ena* mutant and no lethality when fed to wild type. The latter clone was identified as *wve-1*, the *C. elegans* homolog of SCAR/WAVE proteins, which are members of the WASP protein family (Figure 1A; MIKI *et al.* 1998b). Although *wve-1* RNAi feeding to wild type produced no lethality, injection of *wve-1* dsRNA produced ~39% lethality (Figure 2A and our unpublished results). Either feeding or injection of *wve-1* dsRNA produced nearly 100% embryonic lethality in an *unc-34/ena* mutant (Figure 2A and our unpublished results). We also found that either feeding or injection of *wve-1* dsRNA produced nearly complete embryonic lethality in the *wsp-1* mutant (Figure 2A).

Next, we utilized 4D microscopy to examine wild-type, *wsp-1*, or *unc-34/ena* embryos treated with *wve-1* RNAi. Injection of *wve-1* dsRNA into wild-type embryos resulted in a lethality that was similar, but not identical to, the *wsp-1* failure in hypodermal enclosure. The *wve-1* RNAi embryos displayed a disorganized ventral surface, including large, persistent, and sometimes misplaced ventral clefts prior to enclosure and a failure of hypodermal cells to migrate properly to enclose the embryo (Figure 3). Thus, *wve-1* is required for proper enclosure and also displays earlier defects in organization of the embryonic ventral surface. Injection of *wve-1* dsRNA into *unc-34/ena* or *wsp-1* mutant animals resulted in nearly complete embryonic lethality and a severely disorganized ventral surface that exhibited large, misplaced, and persistent ventral clefts (Figures 2 and 3). The hypodermal cells of these embryos failed to migrate and enclose properly (Figure 3). We conclude that *wve-1* RNAi enhances the morphogenesis defects of *wsp-1* mutants and uncovers a role for *unc-34/ena* in morphogenesis revealed only in the absence of either *wsp-1* or *wve-1*.

***wve-1* and *wsp-1* play roles in neuronal development:** Mutations in *unc-34/ena* cause widespread defects in neuronal cell migration and axon outgrowth (DESAI *et al.* 1988; MCINTIRE *et al.* 1992; FORRESTER and GARRIGA 1997). Because WSP-1 and WVE-1 masked the function of UNC-34/Ena in embryogenesis, we analyzed embryos with reduced levels of WSP-1 or WVE-1 for defects in neuronal cell migration and axon outgrowth.

Neither *wsp-1* mutants nor *wsp-1* RNAi-treated embryos displayed defects in the neuronal cell migrations or axon morphologies that we analyzed ($P < 0.0001$, two-tailed *z*-test; Figure 5 and MATERIALS AND METHODS). Although *wsp-1* RNAi treatment of *unc-34/ena* null mutants resulted in nearly complete lethality, *wsp-1* RNAi treatment of the *unc-34/ena* partial loss-of-function mutant *unc-34(e315)* resulted in a number of escapers that could be scored as larvae for defects in cell migration and axon outgrowth. We found that *wsp-1* RNAi treatment of this *unc-34/ena* mutant resulted in a significant enhancement of the neuronal cell migration but not of the axon outgrowth defects ($P < 0.0001$, two-tailed *z*-test; Figure 5 and data not shown).

wve-1 RNAi treatment of wild-type animals resulted in a moderate level of both neuronal cell migration and axon outgrowth defects ($P < 0.0001$, two-tailed *z*-test; Figures 5 and 6). Once again, we were unable to obtain sufficient numbers of viable larvae after *wve-1* RNAi treatment of either *wsp-1* or *unc-34/ena* null mutants to score the effect on neuronal cell migration and axon outgrowth. *wve-1* RNAi treatment of the *unc-34/ena* partial loss-of-function mutant *unc-34(e315)* failed to significantly enhance the neuronal cell migration and axon outgrowth defects (Figures 5 and 6). Surprisingly, feeding *wve-1* dsRNA to wild-type embryos appeared to produce a slightly more severe cell migration defect than when fed to *unc-34*(*e315*); however, the difference between *wve-1* RNAi in wild type and *unc-34(e315)* was not nearly as significant as the differences discussed above ($P = 0.02$ *vs.* $P < 0.0001$; Figure 5). We conclude

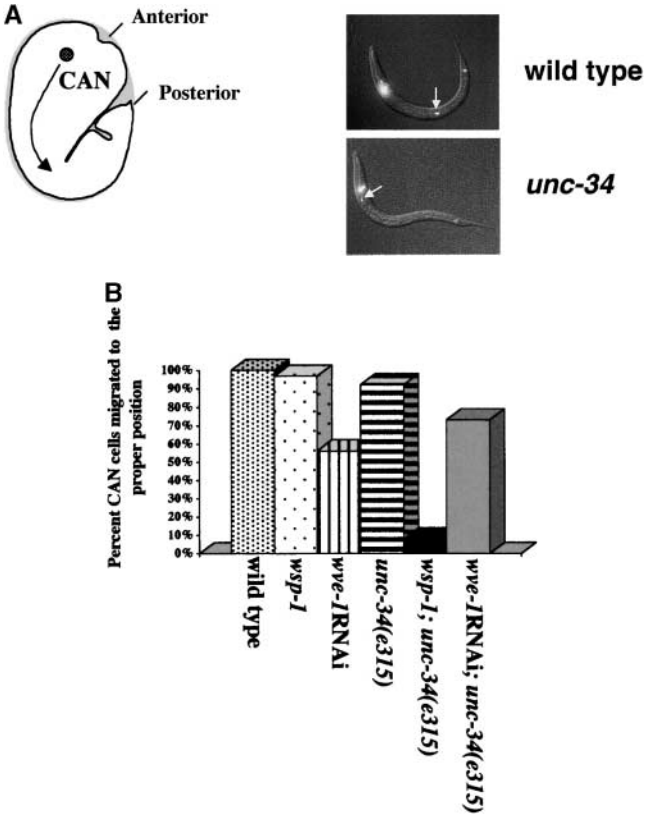

FIGURE 5.—*wsp-1*, *wve-1*, and *unc-34*/Ena function in neuronal cell migration. (A, left) Diagram of the CAN cell embryonic migration route. The CAN is borne in the anterior of the embryo and migrates posteriorly to a position near the middle of the embryo (SULSTON *et al.* 1983). (Right) Examples of CAN cell position using a GFP reporter in wild type and migration mutant (see MATERIALS AND METHODS for details). The CAN cell is positioned near the center of the larva in wild-type animals while it remains more anterior in an *unc-34* mutant (arrow). (B) Histogram displaying the percentage of properly migrated CAN cells in wild-type, *wsp-1*, *wve-1* RNAi, *unc-34(e315)*, *wsp-1* RNAi; *unc-34(e315)*, and *wve-1* RNAi; *unc-34(e315)* animals. All $N \geq 40$. CAN cell position scored as described in MATERIALS AND METHODS.

that *wve-1* plays a role in neuronal cell migration and axon outgrowth while *wsp-1* plays a role in neuronal cell migration normally masked by *unc-34/ena*.

DISCUSSION

WASP and Ena/VASP proteins play overlapping roles during *C. elegans* morphogenesis: The first cell movements of *C. elegans* embryogenesis occur at the 28-cell stage with the ingression of two gut precursor cells (SULSTON *et al.* 1983). Throughout gastrulation groups of cells ingress on the ventral surface of the embryo, leaving behind surface gaps or clefts that are closed by neighboring cells. The most persistent of these clefts, often referred to as the ventral cleft, is formed when a group of MS descendants ingress (SULSTON *et al.* 1983; NANCE and PRIESS 2002). After gastrulation, morphogenesis continues when hypodermal cells migrate from the dorsal side of the embryo to the ventral midline and form adherens junctions in a process known as ventral or hypodermal enclosure (WILLIAMS-MASSON *et al.* 1997, 1998). Once ventral enclosure is complete, circumferential actin rings constrict the ovoid embryo into the vermiform shape of the worm in a process known as elongation (PRIESS and HIRSH 1986).

Several genes that affect ventral enclosure have been identified and can be grouped into different classes on the basis of the process that they affect. One group affects the differentiation of hypodermal cells and includes the transcription factor LIN-26 (QUINTIN *et al.* 2001). A second group includes a cadherin and two catenins required for adhesion of hypodermal cells at the ventral midline (COSTA *et al.* 1998). A third group, which includes ephrins and an ephrin receptor, act from the neuroblasts that cover the embryo's ventral surface prior to morphogenesis and are required for proper closure of the ventral cleft during gastrulation (GEORGE *et al.* 1998; CHIN-SANG *et al.* 1999, 2002). Since mutations in this latter group also confer serious defects in hypodermal cell migration and adhesion, GEORGE *et al.* (1998) proposed that ventral cleft closure and/or an unknown signal from the underlying neuroblasts to the hypodermal cells is required for proper ventral enclosure.

We report here that three actin-remodeling proteins play overlapping roles in these morphogenetic events. First, we observed that *wsp-1* mutant embryos exhibited large, persistent ventral clefts and a subsequent failure of ventral enclosure (Figure 3). Thus, *wsp-1* is required for proper execution of both gastrulation and ventral enclosure. Interestingly, previous work implicated *wsp-1* in hypodermal cell migration during ventral enclosure (SAWA *et al.* 2003). Considering our results with the evidence presented by SAWA *et al.* (2003), we conclude that *wsp-1* plays a role in ventral cleft closure during gastrulation and a later role in hypodermal cell migration during ventral enclosure.

Although *unc-34/ena* mutants displayed no defects in morphogenesis, removing *wsp-1* from an *unc-34/ena* mutant increased the embryonic lethality to 100% (Figure 2). In addition to increasing the frequency of failed ventral enclosures, the size and persistence of the ventral cleft in *wsp-1* mutant embryos was greatly enhanced by *unc-34/ena* mutations (Figure 3). Thus, UNC-34/Ena plays a role in morphogenesis that is revealed only in the absence of WSP-1 function.

Finally, we identified a *C. elegans* homolog of SCAR/WAVE proteins, *wve-1*, on the basis of its requirement for embryonic viability in an *unc-34/ena* mutant background. Injection of *wve-1* dsRNA produced ~30% embryonic lethality (Figure 2). Examination of *wve-1* RNAi-treated embryos revealed a disorganized ventral surface and a failure of hypodermal cells to properly migrate and enclose the embryo. Although injection of *wve-1* dsRNA conferred 30% lethality, feeding of *wve-1* dsRNA

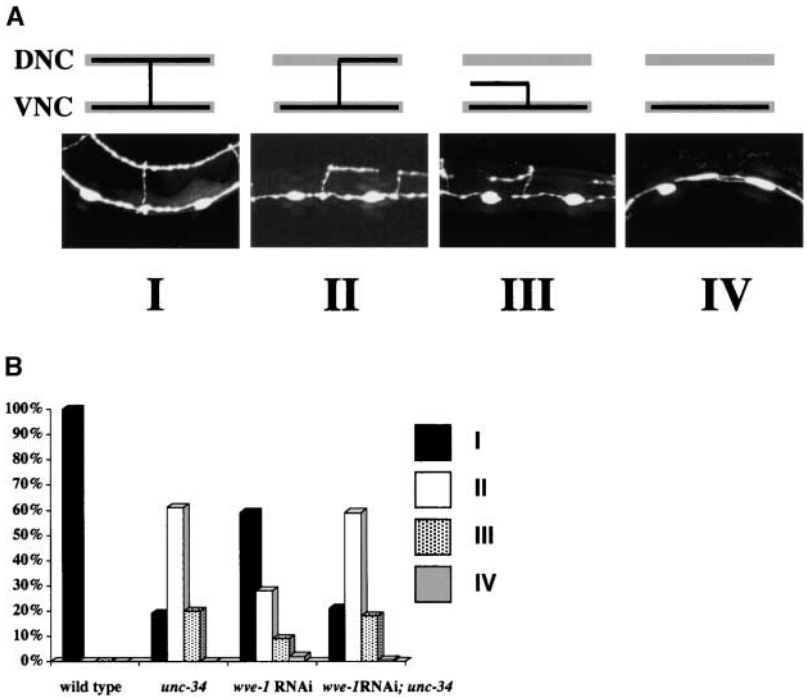

FIGURE 6.—DD motor neuron guidance defects in *unc-34*, *wve-1* RNAi, and *wve-1* RNAi; *unc-34* mutants. (A, top) Diagrams of the four classes of neuronal processes observed. Class I is wild-type morphology. Motor neuron process exits the ventral nerve cord (VNC) and extends along a circumferential commisure to the dorsal nerve cord (DNC) where it branches both anteriorly and posteriorly. Class II processes reach the DNC but fail to branch either anteriorly or posteriorly. Class III processes exit the VNC but fail to reach the DNC, often branching at a more lateral position. Class IV processes fail to exit the VNC. (Bottom) Confocal images of the four motor axon classes using a GFP reporter (see MATERIALS AND METHODS). (B) Histogram displaying percentages of each of the four morphologies in wild type, *unc-34(e315)*, *wve-1* RNAi, and *wve-1* RNAi; *unc-34(e315)* animals. $N \geq 40$ for each genotype. The hypomorphic *unc-34* allele *unc-34(e315)* was utilized in these experiments because the *unc-34* null does not survive to the larval stage required to score motor neuron processes when treated with either *wsp-1* or *wve-1* RNAi (see RESULTS). Process morphology was scored as described in MATERIALS AND METHODS.

produced no lethality (Figure 1 and MATERIALS AND METHODS). Strikingly, feeding or injection of *wve-1* dsRNA into either *unc-34/ena* or *wsp-1* produced nearly 100% embryonic lethality (Figure 2 and our unpublished results). 4D microscopy demonstrated that *wve-1* RNAi; *wsp-1* and *wve-1* RNAi; *unc-34/ena* embryos exhibited severe defects in ventral organization and enclosure (Figure 3).

We propose two nonexclusive models to account for our observations: (1) *wsp-1*, *wve-1*, and *unc-34/ena* play overlapping roles required for proper ventral cleft closure and this leads to a failure in hypodermal cell migration during ventral enclosure, and (2) these genes have independent roles in both ventral cleft closure and ventral enclosure. Consistent with either of the above models, we observed a range of hypodermal cell migrations in embryos that failed to enclose properly. Some embryos exhibited hypodermal migration to the ventral midline and separated during elongation while others failed to reach the ventral midline. Although hypodermal cell migration is known to depend on actin remodeling, much less is known about the cell movements required for ventral cleft closure during gastrulation (WILLIAMS-MASSON *et al.* 1997). Given the known roles of WASP and Ena/VASP proteins in actin remodeling, we were surprised to find that the neuroblast cells that close the ventral cleft do not undergo any gross changes in morphology or actin reorganization during cleft closure (our unpublished observations). Furthermore, the overall actin structure of all mutant combinations examined here were indistinguishable from wild type (our unpublished results). These results are consistent with those reported by SAWA *et al.* (2003) who also failed to observe any perturbations in the gross actin morphology of *wsp-1* RNAi embryos. Nevertheless, our results implicate three actin-remodeling proteins in the process of ventral cleft closure and point to an important role for actin remodeling in this process. Future experiments aimed at deciphering the role of actin in ventral cleft closure may lead to a greater understanding of the mechanisms underlying the process.

***wsp-1*, *wve-1*, and *unc-34/ena* in nervous system development:** Ena /VASP proteins play an important role in development of vertebrate, insect, and nematode nervous systems (MCINTIRE *et al.* 1992; GERTLER *et al.* 1995; LANIER *et al.* 1999). Consistent with these observations, *unc-34/ena* mutants exhibit widespread defects in neuronal cell migration and axon outgrowth (DESAI *et al.* 1988; MCINTIRE *et al.* 1992; FORRESTER and GARRIGA 1997; YU *et al.* 2002). In light of the overlapping roles that *wsp-1* and *wve-1* play with *unc-34/ena* during embryogenesis, we examined their respective roles in nervous system development. Neither *wsp-1* RNAi-treated animals nor the *wsp-1* mutant display defects in neuronal cell migration or axon outgrowth (Figure 4 and our unpublished results). *wsp-1* RNAi treatment of a weak *unc-34/ena* mutant, however, caused a significant enhancement of neuronal cell migration defects (Figure 4). In contrast, *wve-1* RNAi treatment induced defects in both neuronal cell migration and axon outgrowth that were not enhanced by the weak *unc-34/ena* mutation (Figures 4B and 5B).

WASP proteins have been implicated in cell migration in other systems but never shown to affect neuronal cell migration *in vivo* (MIKI *et al.* 1998a; YAMAGUCHI *et al.* 2002). Our findings provide a possible explanation for these results. WASP proteins may function in neuronal

migration in other systems but this role might be masked by the activity of Ena/VASP proteins. SCAR/WAVE mutants, by contrast, have been shown to have defects in cell migration and axon outgrowth in mice and flies, respectively (Zallen *et al.* 2002; Yamazaki *et al.* 2003). Our findings that *wve-1* RNAi causes defects in neuronal cell migration and axon outgrowth are consistent with a conserved role for SCAR/WAVE proteins in these processes.

Role of *wsp-1* in cytokinesis: We report here that a *wsp-1* mutant displays a cytokinesis defect in ~10% of embryos. In some embryos cytokinesis failed at the first embryonic division while in others we observed the failure as late as 16–24 cells (Figure 4A and our unpublished results). Because cell boundaries become increasingly difficult to observe as the embryo matures, we do not know at this time whether *wsp-1* is required only for cytokinesis in the early embryo.

Interestingly, other actin-regulating proteins have previously been shown to play a role in *C. elegans* cytokinesis (Severson *et al.* 2002). A conserved aspect of cytokinesis is the formation of an actinomyosin contractile ring required to generate the forces necessary for cell separation (Scholey *et al.* 2003). Recent work in fission yeast demonstrated a role for WASP-mediated actin polymerization within the contractile ring (Pelham and Chang 2002; Rajagopalan *et al.* 2003). Although WASP is not absolutely required for cytokinesis in yeast, the contractile ring of *wsp1* mutant cells constricts more slowly than in wild type (Pelham and Chang 2002). Interestingly, cortical actin morphology and abundance in the *wsp-1* mutant embryos was indistinguishable from wild type (our unpublished results). Further experiments are required to define the exact role of WSP-1 in cytokinesis but one possibility is that it is required for the optimal rate of contractile ring closure and that this leads to a low rate of failure in cell division.

Overlapping roles of WASP and Ena/VASP proteins in *C. elegans*: Although WASP and Ena/VASP family proteins are both known to regulate actin dynamics, little is known about how they might interact functionally *in vivo*. Our work provides *in vivo* evidence that three distinct actin-remodeling proteins from two different protein families play overlapping roles during embryogenesis and nervous system development. SCAR/WAVE and WASP proteins both catalyze the formation of new actin filaments through the ARP2/3 complex (Pollard *et al.* 2001; Badour *et al.* 2003; Carlier *et al.* 2003). Despite sharing this activity, SCAR and WASP proteins are regulated by different mechanisms and are known to be required for distinct processes. Given the distinct regulatory mechanisms of WASP and SCAR proteins, it seems unlikely that they play redundant roles during *C. elegans* morphogenesis. Further experiments will be required to determine whether they act in the same cellular process or independently in separate processes during the same stage of embryogenesis.

Ena/VASP proteins have been shown to promote F-actin elongation through an ARP2/3 independent mechanism (Bear *et al.* 2002); however, WASP and VASP proteins interact *in vitro* and VASP may be required for WASP to activate the ARP2/3 complex at the periphery of hemopoietic cells (Castellano *et al.* 2001). Our results demonstrate that UNC-34/Ena, WSP-1, and WVE-1 play overlapping roles during embryogenesis and neuronal cell migration. These observations provide new insight into the function of WASP and Ena/VASP proteins and lay the foundation for future experiments to determine whether UNC-34/Ena and WSP-1 act independently or cooperatively. It may be that UNC-34/Ena affects actin dynamics independently of WSP-1 and WVE-1 but sufficient actin remodeling occurs to promote morphogenesis in the absence of UNC-34/Ena as long as the ARP2/3 complex is activated. Alternatively, UNC-34/Ena may act from within the same process or protein complex as WSP-1 and/or WVE-1 but (may) not be essential for function as long as either WSP-1 or WVE-1 is present. For instance, UNC-34/Ena could be required for the optimal rate of actin polymerization of new free ends created by ARP2/3 activation or for competing with capping proteins to create free ends usable for ARP2/3-mediated filament branching. *C. elegans* provides a simple genetic system in which to study the overlapping roles of *unc-34/ena*, *wsp-1*, and *wve-1*, and because Ena/VASP and WASP family proteins are evolutionarily conserved, any cellular processes or protein complexes defined in *C. elegans* are likely to be conserved as well.

We thank Jeff Hardin for help characterizing the morphogenesis defects in *wsp-1* RNAi; *unc-34* mutant embryos and for useful discussion, Aaron Severson for critical reading of the manuscript, and members of the Garriga lab for helpful discussion and suggestions. We also thank Yuji Kohara for cDNA clones used in this study. This work was supported by grants to G.G. from the National Institutes of Health (NS32057). J.W. and N.H. were supported by the American Cancer Society.

LITERATURE CITED

Ahern-Djamali, S. M., A. R. Comer, C. Bachmann, A. S. Kastenmeier, S. K. Reddy *et al.*, 1998 Mutations in Drosophila enabled and rescue by human vasodilator-stimulated phosphoprotein (VASP) indicate important functional roles for Ena/VASP homology domain 1 (EVH1) and EVH2 domains. Mol. Biol. Cell **9:** 2157–2171.

Amann, K. J., and T. D. Pollard, 2001 The Arp2/3 complex nucleates actin filament branches from the sides of pre-existing filaments. Nat. Cell Biol. **3:** 306–310.

Aspenstrom, P., U. Lindberg and A. Hall, 1996 Two GTPases, Cdc42 and Rac, bind directly to a protein implicated in the immunodeficiency disorder Wiskott-Aldrich syndrome. Curr. Biol. **6:** 70–75.

Bachmann, C., L. Fischer, U. Walter and M. Reinhard, 1999 The EVH2 domain of the vasodilator-stimulated phosphoprotein mediates tetramerization, F-actin binding, and actin bundle formation. J. Biol. Chem. **274:** 23549–23557.

Badour, K., J. Zhang and K. A. Siminovitch, 2003 The Wiskott-Aldrich syndrome protein: forging the link between actin and cell activation. Immunol. Rev. **192:** 98–112.

Bashaw, G. J., T. Kidd, D. Murray, T. Pawson and C. S. Goodman, 2000 Repulsive axon guidance: Abelson and Enabled play op-

posing roles downstream of the roundabout receptor. Cell **101:** 703–715.

Bear, J. E., T. M. Svitkina, M. Krause, D. A. Schafer, J. J. Loureiro *et al.*, 2002 Antagonism between Ena/VASP proteins and actin filament capping regulates fibroblast motility. Cell **109:** 509–521.

Blanchoin, L., K. J. Amann, H. N. Higgs, J. B. Marchand, D. A. Kaiser *et al.*, 2000 Direct observation of dendritic actin filament networks nucleated by Arp2/3 complex and WASP/Scar proteins. Nature **404:** 1007–1011.

Brenner, S., 1974 The genetics of *Caenorhabditis elegans*. Genetics **77:** 71–94.

Carlier, M. F., C. Le Clainche, S. Wiesner and D. Pantaloni, 2003 Actin-based motility: from molecules to movement. BioEssays **25:** 336–345.

Castellano, F., C. Le Clainche, D. Patin, M. F. Carlier and P. Chavrier, 2001 A WASp-VASP complex regulates actin polymerization at the plasma membrane. EMBO J. **20:** 5603–5614.

Chin-Sang, I. D., and A. D. Chisholm, 2000 Form of the worm: genetics of epidermal morphogenesis in C. elegans. Trends Genet. **16:** 544–551.

Chin-Sang, I. D., S. E. George, M. Ding, S. L. Moseley, A. S. Lynch *et al.*, 1999 The ephrin VAB-2/EFN-1 functions in neuronal signaling to regulate epidermal morphogenesis in C. elegans. Cell **99:** 781–790.

Chin-Sang, I. D., S. L. Moseley, M. Ding, R. J. Harrington, S. E. George *et al.*, 2002 The divergent C. elegans ephrin EFN-4 functions in embryonic morphogenesis in a pathway independent of the VAB-1 Eph receptor. Development **129:** 5499–5510.

Costa, M., W. Raich, C. Agbunag, B. Leung, J. Hardin *et al.*, 1998 A putative catenin-cadherin system mediates morphogenesis of the Caenorhabditis elegans embryo. J. Cell Biol. **141:** 297–308.

Desai, C., G. Garriga, S. L. McIntire and H. R. Horvitz, 1988 A genetic pathway for the development of the Caenorhabditis elegans HSN motor neurons. Nature **336:** 638–646.

Forrester, W. C., and G. Garriga, 1997 Genes necessary for C. elegans cell and growth cone migrations. Development **124:** 1831–1843.

Fraser, A. G., R. S. Kamath, P. Zipperlen, M. Martinez-Campos, M. Sohrmann *et al.*, 2000 Functional genomic analysis of C. elegans chromosome I by systematic RNA interference. Nature **408:** 325–330.

George, S. E., K. Simokat, J. Hardin and A. D. Chisholm, 1998 The VAB-1 Eph receptor tyrosine kinase functions in neural and epithelial morphogenesis in C. elegans. Cell **92:** 633–643.

Gertler, F. B., J. S. Doctor and F. M. Hoffmann, 1990 Genetic suppression of mutations in the Drosophila abl proto-oncogene homolog. Science **248:** 857–860.

Gertler, F. B., A. R. Comer, J. L. Juang, S. M. Ahern, M. J. Clark *et al.*, 1995 enabled, a dosage-sensitive suppressor of mutations in the Drosophila Abl tyrosine kinase, encodes an Abl substrate with SH3 domain-binding properties. Genes Dev. **9:** 521–533.

Gertler, F. B., K. Niebuhr, M. Reinhard, J. Wehland and P. Soriano, 1996 Mena, a relative of VASP and Drosophila Enabled, is implicated in the control of microfilament dynamics. Cell **87:** 227–239.

Harrington, R. J., M. J. Gutch, M. O. Hengartner, N. K. Tonks and A. D. Chisholm, 2002 The C. elegans LAR-like receptor tyrosine phosphatase PTP-3 and the VAB-1 Eph receptor tyrosine kinase have partly redundant functions in morphogenesis. Development **129:** 2141–2153.

Kwiatkowski, A. V., F. B. Gertler and J. J. Loureiro, 2003 Function and regulation of Ena/VASP proteins. Trends Cell Biol. **13:** 386–392.

Lanier, L. M., M. A. Gates, W. Witke, A. S. Menzies, A. M. Wehman *et al.*, 1999 Mena is required for neurulation and commissure formation. Neuron **22:** 313–325.

Laurent, V., T. P. Loisel, B. Harbeck, A. Wehman, L. Grobe *et al.*, 1999 Role of proteins of the Ena/VASP family in actin-based motility of Listeria monocytogenes. J. Cell Biol. **144:** 1245–1258.

McIntire, S. L., G. Garriga, J. White, D. Jacobson and H. R. Horvitz, 1992 Genes necessary for directed axonal elongation or fasciculation in C. elegans. Neuron **8:** 307–322.

Miki, H., S. Nonoyama, Q. Zhu, A. Aruffo, H. D. Ochs *et al.*, 1997 Tyrosine kinase signaling regulates Wiskott-Aldrich syndrome protein function, which is essential for megakaryocyte differentiation. Cell Growth Differ. **8:** 195–202.

Miki, H., T. Sasaki, Y. Takai and T. Takenawa, 1998a Induction of filopodium formation by a WASP-related actin-depolymerizing protein N-WASP. Nature **391:** 93–96.

Miki, H., S. Suetsugu and T. Takenawa, 1998b WAVE, a novel WASP-family protein involved in actin reorganization induced by Rac. EMBO J. **17:** 6932–6941.

Nance, J., and J. R. Priess, 2002 Cell polarity and gastrulation in C. elegans. Development **129:** 387–397.

Niebuhr, K., F. Ebel, R. Frank, M. Reinhard, E. Domann *et al.*, 1997 A novel proline-rich motif present in ActA of Listeria monocytogenes and cytoskeletal proteins is the ligand for the EVH1 domain, a protein module present in the Ena/VASP family. EMBO J. **16:** 5433–5444.

Pantaloni, D., R. Boujemaa, D. Didry, P. Gounon and M. F. Carlier, 2000 The Arp2/3 complex branches filament barbed ends: functional antagonism with capping proteins. Nat. Cell Biol. **2:** 385–391.

Pelham, R. J., and F. Chang, 2002 Actin dynamics in the contractile ring during cytokinesis in fission yeast. Nature **419:** 82–86.

Pollard, T. D., L. Blanchoin and R. D. Mullins, 2000 Molecular mechanisms controlling actin filament dynamics in nonmuscle cells. Annu. Rev. Biophys. Biomol. Struct. **29:** 545–576.

Pollard, T. D., L. Blanchoin and R. D. Mullins, 2001 Actin dynamics. J. Cell Sci. **114:** 3–4.

Prehoda, K. E., D. J. Lee and W. A. Lim, 1999 Structure of the enabled/VASP homology 1 domain-peptide complex: a key component in the spatial control of actin assembly. Cell **97:** 471–480.

Priess, J. R., and D. I. Hirsh, 1986 Caenorhabditis elegans morphogenesis: the role of the cytoskeleton in elongation of the embryo. Dev. Biol. **117:** 156–173.

Quintin, S., G. Michaux, L. McMahon, A. Gansmuller and M. Labouesse, 2001 The Caenorhabditis elegans gene lin-26 can trigger epithelial differentiation without conferring tissue specificity. Dev. Biol. **235:** 410–421.

Rajagopalan, S., V. Wachtler and M. Balasubramanian, 2003 Cytokinesis in fission yeast: a story of rings, rafts and walls. Trends Genet. **19:** 403–408.

Ramesh, N., I. M. Anton, J. H. Hartwig and R. S. Geha, 1997 WIP, a protein associated with Wiskott-Aldrich syndrome protein, induces actin polymerization and redistribution in lymphoid cells. Proc. Natl. Acad. Sci. USA **94:** 14671–14676.

Reinhard, M., K. Giehl, K. Abel, C. Haffner, T. Jarchau *et al.*, 1995 The proline-rich focal adhesion and microfilament protein VASP is a ligand for profilins. EMBO J. **14:** 1583–1589.

Reinhard, M., T. Jarchau and U. Walter, 2001 Actin-based motility: stop and go with Ena/VASP proteins. Trends Biochem. Sci. **26:** 243–249.

Rivero-Lezcano, O. M., A. Marcilla, J. H. Sameshima and K. C. Robbins, 1995 Wiskott-Aldrich syndrome protein physically associates with Nck through Src homology 3 domains. Mol. Cell. Biol. **15:** 5725–5731.

Rohatgi, R., H. Y. Ho and M. W. Kirschner, 2000 Mechanism of N-WASP activation by CDC42 and phosphatidylinositol 4, 5-bisphosphate. J. Cell Biol. **150:** 1299–1310.

Sawa, M., S. Suetsugu, A. Sugimoto, H. Miki, M. Yamamoto *et al.*, 2003 Essential role of the C. elegans Arp2/3 complex in cell migration during ventral enclosure. J. Cell Sci. **116:** 1505–1518.

Scholey, J. M., I. Brust-Mascher and A. Mogilner, 2003 Cell division. Nature **422:** 746–752.

Severson, A. F., D. L. Baillie and B. Bowerman, 2002 A formin homology protein and a profilin are required for cytokinesis and Arp2/3-independent assembly of cortical microfilaments in C. elegans. Curr. Biol. **12:** 2066–2075.

Simmer, F., C. Moorman, A. M. Van Der Linden, E. Kuijk, P. V. Van Den Berghe *et al.*, 2003 Genome-wide RNAi of C. elegans using the hypersensitive rrf-3 strain reveals novel gene functions. PLoS Biol. **1:** E12.

Simske, J. S., and J. Hardin, 2001 Getting into shape: epidermal morphogenesis in Caenorhabditis elegans embryos. BioEssays **23:** 12–23.

Suetsugu, S., H. Miki and T. Takenawa, 1999a Distinct roles of profilin in cell morphological changes: microspikes, membrane ruffles, stress fibers, and cytokinesis. FEBS Lett. **457:** 470–474.

Suetsugu, S., H. Miki and T. Takenawa, 1999b Identification of two human WAVE/SCAR homologues as general actin regulatory molecules which associate with the Arp2/3 complex. Biochem. Biophys. Res. Commun. **260:** 296–302.

Suetsugu, S., H. Miki and T. Takenawa, 2002 Spatial and temporal

regulation of actin polymerization for cytoskeleton formation through Arp2/3 complex and WASP/WAVE proteins. Cell Motil. Cytoskeleton **51:** 113–122.

Sulston, J. E., E. Schierenberg, J. G. White and J. N. Thomson, 1983 The embryonic cell lineage of the nematode Caenorhabditis elegans. Dev. Biol. **100:** 64–119.

Symons, M., J. M. Derry, B. Karlak, S. Jiang, V. Lemahieu *et al.*, 1996 Wiskott-Aldrich syndrome protein, a novel effector for the GTPase CDC42Hs, is implicated in actin polymerization. Cell **84:** 723–734.

Timmons, L., D. L. Court and A. Fire, 2001 Ingestion of bacterially expressed dsRNAs can produce specific and potent genetic interference in Caenorhabditis elegans. Gene **263:** 103–112.

Vasioukhin, V., C. Bauer, M. Yin and E. Fuchs, 2000 Directed actin polymerization is the driving force for epithelial cell-cell adhesion. Cell **100:** 209–219.

Wightman, B., S. G. Clark, A. M. Taskar, W. C. Forrester, A. V. Maricq *et al.*, 1996 The C. elegans gene vab-8 guides posteriorly directed axon outgrowth and cell migration. Development **122:** 671–682.

Williams-Masson, E. M., A. N. Malik and J. Hardin, 1997 An actin-mediated two-step mechanism is required for ventral enclosure of the C. elegans hypodermis. Development **124:** 2889–2901.

Williams-Masson, E. M., P. J. Heid, C. A. Lavin and J. Hardin, 1998 The cellular mechanism of epithelial rearrangement during morphogenesis of the Caenorhabditis elegans dorsal hypodermis. Dev. Biol. **204:** 263–276.

Yamaguchi, H., H. Miki and T. Takenawa, 2002 Neural Wiskott-Aldrich syndrome protein is involved in hepatocyte growth factor-induced migration, invasion, and tubulogenesis of epithelial cells. Cancer Res. **62:** 2503–2509.

Yamazaki, D., S. Suetsugu, H. Miki, Y. Kataoka, S. Nishikawa *et al.*, 2003 WAVE2 is required for directed cell migration and cardiovascular development. Nature **424:** 452–456.

Yu, T. W., J. C. Hao, W. Lim, M. Tessier-Lavigne and C. I. Bargmann, 2002 Shared receptors in axon guidance: SAX-3/Robo signals via UNC-34/Enabled and a Netrin-independent UNC-40/DCC function. Nat. Neurosci. **5:** 1147–1154.

Zallen, J. A., Y. Cohen, A. M. Hudson, L. Cooley, E. Wieschaus *et al.*, 2002 SCAR is a primary regulator of Arp2/3-dependent morphological events in Drosophila. J. Cell Biol. **156:** 689–701.

Communicating editor: K. Kemphues